NASA Contractor Report 185116

Two-Dimensional High Temperature Optical Strain Measurement System—Phase II

Christian T. Lant

Sverdrup Technology, Inc.
NASA Lewis Research Center Group
Cleveland, Ohio

July 1989

Prepared for
Lewis Research Center
Under Contract NAS3-25266

National Aeronautics and
Space Administration

TWO-DIMENSIONAL HIGH TEMPERATURE OPTICAL STRAIN MEASUREMENT SYSTEM - PHASE II

Christian T. Lant
Sverdrup Technology, Inc.
NASA Lewis Research Center Group
Cleveland, Ohio 44135

1. SUMMARY

The work performed under this contract covered the second phase of a multiphase effort in developing an optical strain measurement system capable of mapping in two dimensions the strain on the surface of a hot specimen. The objective of this Phase II work has been to provide a noncontact, two-dimensional differential strain gauge for use in a high temperature experimental test facility.

The optical strain measurement system developed in this Phase II effort builds upon the results of the Phase I one-dimensional system (ref. 1). The basic optical technique used in both the Phase I and Phase II systems is based on the work of I. Yamaguchi (ref. 2). The displacement of speckle patterns generated by a test specimen subject to stress is directly proportional to surface strain. The use of two symmetrically incident laser beams allows automatic cancellation of speckle translation terms due to rigid body motion. The measurements are made automatically under control of a microcomputer. The speckle pattern shifts are calculated by cross-correlating one-dimensional speckle patterns recorded on a linear photodiode array before and after strain. The sensitive axis of the gauge is determined by the incident plane of the laser beams. By rotating the incident plane, different components of strain can be measured. The principal strains at a point on the specimen are calculated after measuring three components of surface strain.

Accurate one- and two-dimensional stress-strain plots have been generated. Linear strain relationships have been demonstrated at specimen temperatures up to 750 °C. The resolution of the optical system is 15 microstrain using the current configuration, and the one-dimensional strain measurement error is ±15 $\mu\epsilon$ ±0.9 percent of the strain reading. The two-dimensional measurements have a maximum theoretical error of three times the one-dimensional error. It has been observed that the test equipment led to imprecise loading of the specimen, and contributed to some of the errors encountered.

2. INTRODUCTION

2.1 Program

Investigations of physical phenomena affecting the durability of Space Shuttle Main Engine (SSME) components require the development of measurement systems operable in hostile environments. The need for such instrumentation defined this program to develop a noncontact optical strain measurement system to aid in these investigations. This task is a multiphase effort designed to provide two-dimensional measurements of principal strains on the surface of a hot specimen. Sverdrup Technology, Inc. is developing this in-house system at the facilities of NASA Lewis Research Center's Instrumentation and Control Technology Division.

2.1.1 Background. - Optical strain measurement techniques share a number of common advantages, as well as a number of common limitations. Specific techniques differ in the way they minimize various limitations as well as augment their strengths, with most filling some gap in the field of instrumentation. The applications of each particular technique are thus dictated by the technique's set of characteristics.

Categorically, optical techniques tend to have a high sensitivity to movement and deformation. This is an advantage in that these parameters can be measured very precisely, however, it also places an upper limit on how much movement and deformation can be tolerated in a test before the signal is lost. Optical techniques also share an immunity to radio frequency interference. Although the electrical components of an optical measurement system are sensitive to RFI, these components can often be located far from the noise source or shielded sufficiently; the optical beam and the transmission medium itself are immune to the RF noise.

A trait common to optical measurement techniques is that all require some form of optical access to the measurement point. In the event that the measurement is taken in an enclosed test environment, the access can be in either the form of a window or an optical waveguide. Further, some situations allow the optical sensor to be mounted within the enclosure.

Optical measurement techniques also differ in many areas. Some, such as speckle interferometry, double exposure holography, and moire, store full field measurements which are probed at a later time for local information. Others take pointwise measurements with high spatial resolution, where the output is obtained in real or near real time. Some techniques require preparation of the surface before a measurement, such as application of a grating, flags, or indentations.

This project is based on a laser speckle strain measurement technique developed by I. Yamaguchi. The technique is completely noncontacting and requires no surface preparation. This allows a test section to be easily mapped with full flexibility in gauge location. Single point measurements are made while automatically correcting for rigid body motion errors, and the technique allows for a near real time output of strain. Optical strain information is, in many techniques, indistinguishable from rigid body motion information; having in this technique the means not only to cancel rigid body motion effects, but to do so automatically, greatly decreases the restrictions placed on a test setup. Strain is calculated by electronically cross-correlating speckle pattern shifts recorded in the diffraction plane.

2.1.2 Objectives. - The first phase of this task demonstrated one-dimensional strain measurement at temperatures up to 450 °C, with a resolution of 18 microstrain. This final report describes the Phase II strain measurement system and the results obtained during the testing period. The objective of the Phase II system is to provide a noncontact, two-dimensional strain gauge for high temperature measurements in an experimental test facility. The Phase II system builds on the results of the one-dimensional Phase I system to demonstrate measurements of the first and second principal strains on the surface of a hot specimen.

The system is designed to determine the principal strain axes at a point (with a gauge length of 0.5 to 1.0 mm), and to be adaptable to mapping the strain field over a specified area of the test specimen. A number of secondary objectives were designed to increase the performance of the system. These include:

(1) Eliminating error sensitivity to out-of-plane motion: By increasing the radius of curvature of the laser beam at the specimen surface, sensitivity to rigid body motion is eliminated.

(2) Increasing temperature measurement range: The stability of the speckle patterns with respect to temperature is increased by surrounding the specimen in a thermally insulating enclosure, and by modifying the optical parameters of the system.

(3) Decreasing computation time per correlation: The speckle correlation time is reduced by increasing the computer hardware performance and/or reducing the number of operations in the correlation algorithm.

3. THEORY

3.1 Speckle Shift Relations

The optical technique used in both the Phase I and Phase II systems relies on the linear relationship between surface strain and laser speckle pattern shifts in the diffraction plane. Laser speckle is a phase effect which occurs when spatially coherent light interacts with a rough surface. Since speckle is generated by any diffusely reflecting surface, no preparation is needed to obtain a good signal. The speckle displacement relations are described well in references 1 and 2.

Referring to figure 3.1.1, a test specimen in the object plane xy is located parallel to a linear photodiode array in the observation plane XY. The observation plane is a distance L_o from the object plane. Applying a load to the specimen deforms the object point O by $\vec{a}(x,y)$. The resulting speckle displacement is denoted by $\vec{A}$.

When a laser beam having a radius of curvature L_s is directed onto the loaded specimen at an angle θ_s, a photodiode array located along the normal to the specimen surface detects objective speckle. This speckle field shifts in response to deformation and rigid body motion of the specimen. The complicated speckle shifts are reduced to a simple relationship involving only the desired component of strain. This simplification is achieved by means of three requirements:

(1) The photodiode array must be oriented parallel to both the incident plane of the beam and the specimen surface;

(2) The laser beam wavefront must be relatively planar at the specimen surface;

(3) Differential speckle shift measurements must be made, using beams incident on the specimen at equal and opposite angles.

There are two speckle shift terms remaining after requirements 1 and 2 are met. Now by taking the difference between the shifts from two beams (requirement 3), the remaining term of rigid body motion is cancelled. The residual differential speckle shift is due only to surface strain parallel to the linear photodiode array, and is given by equation (3.1.1):

$$\epsilon_{xx} = -\Delta A_x \frac{1}{2L_o \sin(\theta)} \qquad (3.1.1)$$

where $\theta \equiv |\theta_s|$, and ΔA_x is the difference between speckle shifts from beam 1 and beam 2.

3.2 Principal Strains

The basic technique described in section 3.1 measures the component of surface strain parallel to the incident plane of the optical system. However, many engineering tests require knowledge of the maximum and minimum strains at a point, and the orientation of these strains on the specimen.

Measurement of these principal strains is typically done using a rosette configuration of bonded resistance strain gauges. Three components of strain are measured at different angles on the specimen, which through a coordinate transformation yield the principal axes of strain and their orientation on the specimen (ref. 3). The transformation is a completely geometric result, and independent of the method used to obtain the strain components. The three sampled components of strain are denoted ϵ_a, ϵ_b, and ϵ_c. For a rectangular rosette configuration (see fig. 3.2.1), the principal strain components ϵ_1 and ϵ_2 and their angle of rotation are given by equations (3.2.1-3):

$$\epsilon_1 = \frac{1}{2}\left[\epsilon_a + \epsilon_c + \sqrt{(2\epsilon_b - \epsilon_a - \epsilon_c)^2 + (\epsilon_c - \epsilon_a)^2}\right] \qquad (3.2.1)$$

$$\epsilon_2 = \frac{1}{2}\left[\epsilon_a + \epsilon_c - \sqrt{(2\epsilon_b - \epsilon_a - \epsilon_c)^2 + (\epsilon_c - \epsilon_a)^2}\right] \qquad (3.2.2)$$

$$\phi = \frac{1}{2}\tan^{-1}\left[\frac{(\epsilon_c - \epsilon_a)}{(2\epsilon_b - \epsilon_a - \epsilon_c)}\right] \qquad (3.2.3)$$

where ϕ is the angle of rotation of the principal strain axes.

Obtaining these three basic components using this optical technique requires the optical incident plane to be rotated quickly and repeatably, without altering the alignment of the system. Due to the finite time needed to rotate the optical assembly, the measurements must be made during relatively static loading of the specimen.

Rotation of the incident plane is achieved by mounting the rotating optical assembly on a goniometer. The specifications of the goniometer maintain the stability requirements of resolution, wobble, and repeatability. Details on the operation of the optical system will be given in section 4.1.

4. SETUP

The Phase II system inherently has many subsystems in common with the Phase I system from which it is derived. This evolution has made it possible to adapt the control architecture developed in Phase I to the requirements of the Phase II system with minimal changes.

There are three fundamental differences between the Phase I and II systems: (1) the optical set up, (2) system software, and (3) the data acquisition/control hardware. These three areas will be explained in detail in the following sections. Reference 1 covers the setup and operation of the remaining unchanged subsystems.

4.1 Optical System

A schematic of the optical system is given in figure 4.1.1. An argon ion laser beam is switched by an acousto-optic modulator (AOM). The zeroth order beam is used as the exposure beam for the line scan camera, and the first order beam is absorbed by the beam stop between exposures. Waist positioning lenses position the laser beam waist onto the specimen surface. Since the wavefront is planar at the waist, requirement 2 in section 3.1 is satisfied.

Polarization sensitive optics are used to provide the symmetrically incident exposure beams for rigid body motion cancellation. A polarization beamsplitting cube transmits the beam to side 1 or reflects it to side 2, depending on the orientation of the polarization vector. An appropriate bias voltage across the Pockels cell allows the polarization vector of the beam to be rotated by 90°, switching the beam from side 1 to side 2. The beam on side 1 is then directed onto the specimen at an angle of +30° from the normal, and the beam redirected onto side 2 is incident at -30°.

As discussed in section 3.2, the sensitive axis of the gauge is defined by the plane of incidence of the laser beams. Rotation of this plane is achieved by mounting the final stage of the beamsteering optics (rotating assembly) on a goniometer cradle, where the goniometer is free to rotate ±45° about its center point. This final stage assembly also contains the linear photodiode array (line scan camera), so that the alignment of the sensor axis with the plane of incidence is always constant. The goniometer has a resolution of ±0.01° using an optical encoder, and the position is programmable by the system computer through an IEEE-488 port on the goniometer controller. In addition to the rotational freedom, a minimum of two more degrees of freedom are required by the system for alignment between the optics and the specimen, these being translations along the X and Z axes. The goniometer is mounted to an X-Z positioner for this alignment.

Using the combination of the Pockels cell and beamsplitting cube to switch the beams makes the entire rotating assembly sensitive to the polarization of the laser beam. At the same time, the rotating assembly must be free to rotate independently from the laser head. To circumvent this problem, two quarter

wave ($\lambda/4$) retardation plates are used to provide rotational invariance for the polarization sensitive optics in the rotating assembly. The first waveplate is stationary, and converts the beam from linear to circular polarization; the second waveplate, mounted in the rotating assembly, converts the beam back to linear polarization. The key point is that the linear polarization vectors are now fixed relative to each of their respective waveplates.

The new design of the optical system introduces a number of advantages over the Phase I design. Switching a single beam along one of two legs allows all of the optical power to be directed into the exposure beam. This reduces the exposure time of the line scan camera by a factor of two, which not only reduces any smearing of moving speckle patterns, but reduces dark current noise levels in the photodiode array. Another advantage is that the size of the optical pallet has also been reduced by a factor of two, making it easier to position the optics in a test cell. In addition, the incident angle of the beams on the specimen has been reduced from 45° to 30°, making optical access to the specimen easier while maintaining the sensitivity of the gauge (L_o has been increased to 1 m).

Figure 4.1.2 is a view of the test setup. The test specimen in a thermal enclosure is shown mounted in a horizontally configured testing machine. The optical setup occupies a 4- by 5-ft section of the optical table. A close-up view of the rotating assembly mounted on the goniometer is shown in figure 4.1.3. The assembly is rotated to angle 'c' (45°) for clarity. The testing machine is seen along the left edge of the figure.

4.2 Software

The basic framework of the Phase I main control program is also used in the Phase II system. The main program is a menu driven program that allows either manual control of procedures or automatic execution of predetermined data acquisition and processing routines. Changes in the Phase II software include the data array structure, enhanced data acquisition menus, added features in the plotting routines, the structure of the correlation software, and the execution speed of the code.

The software is written in Hewlett Packard's HPBASIC language, which is a powerful, fast, and interactive scientific control language. The features of HPBASIC allow for very flexible I/O, data analysis, and display in a structured environment.

To further improve the execution time of the control software in Phase II, a HPBASIC compiler was purchased. In addition, a floating point processor improves the execution times of the calculation intensive routines such as the cross-correlation. The combination of these two improvements enabled the cross-correlations to be performed in HPBASIC rather than using the BASIC callable Pascal routine used in Phase I. The HPBASIC routine is not only faster than the equivalent Pascal routine, but the function calling overhead time is also reduced. The correlation time is presently 50 sec for a two-dimensional measurement; this time represents six correlations, so there is about a factor of two improvement in speed per correlation over Phase I.

Data acquisition software changes include a number of procedural elements designed to minimize the time required to read the speckle patterns, as well as to assure that the load readings correspond as closely as possible to the load at the time the speckle patterns are read. The speckle patterns from beam 1 and beam 2 must be read in close succession so that neither movement of the specimen nor refractive media can occur in the time it takes to record the patterns. By storing both patterns in the waveform recorder buffer before transferring the data to the computer, a few milliseconds are saved between exposures.

4.3 Data Acquisition Hardware

The various components of the system are tied together by a Hewlett Packard 236CU microcomputer. Control is achieved through IEEE-488 interfaces, and a custom electronic control/timing interface. The custom interface is linked to the computer by a digital output card. The function of the custom electronics is to provide an interface for control and data acquisition between the linear photodiode array camera and the system computer. Circuit boards have been designed to programmably select the exposure beam using a Pockels cell, control the exposure time of the camera by means of an acousto-optic modulator and pulse generator, and to read the speckle data into the computer using a waveform recorder. The computer system and control electronics are shown in figure 4.3.1. Some minor changes in the Phase I custom electronics package were necessary to accommodate the different beam control requirements of the Phase II system.

The specific changes in the electronic circuits involve control of the acousto-optic modulator and the Pockels cell. To improve the laser beam characteristics the undeflected laser beam is used as the exposure beam, and the first order (deflected) beam is the default off state of the beam, for safety considerations. The circuit change adds a logical inverter to the input of the AOM control line driver. The Pockels cell is switched by an AOM control circuit modified to isolate it from the camera timing circuitry. The other data acquisition control circuitry is essentially unchanged.

5. TEST PROCEDURES

Three major changes over the Phase I system that require testing are incorporated into the Phase II system. These changes are:

1. The sensitive axis of the gauge is rotatable, providing a two-dimensional strain measurement capability;

2. Provisions are made to increase the temperature range of the gauge;

3. Rigid body motion error is eliminated.

Each item above has been tested and evaluated in the sections to follow.

5.1 Two-Dimensional Strain

The ability to calculate the first and second principal strains from three components of surface strain is the most challenging feature of this system. The alignment, positioning, and repeatability requirements are all very stringent, and are necessary for the success of the measurements.

A few requirements are necessary to insure good correlation between the reference and shifted speckle patterns. First of all, the rotation of the goniometer must be accurate and repeatable to within 0.5 mrad for correlation to occur. The reference and shifted spot locations should also be coincident to within 50 percent of the spot diameter. The output mode of the laser beam provides a spot size ω (diameter) of 0.6 mm; this limits the wobble of the goniometer to less than 0.3 mrad.

The alignment of the optical system must prevent both laser spots from deviating from the gauge position on the specimen as the sensitive axis is rotated. This is critical in assuring that the integrity of the gauge length and position is maintained, for the assumption when using a very short gauge length is that the surface strain is not uniform. The spatial resolution of the system is lost if the spots move during the measurement.

In addition, the reference speckle pattern must be updated often enough to counter drift of the pattern off of the photodiode array due to rigid body motion as the specimen is loaded. The results presented in section 6 were obtained using the incremental shift technique (ref. 4), where the reference patterns are updated before each load increment.

Alignment of the rotating assembly in order to maintain requirements 1 through 3 in section 3.1 is a critical factor not only in obtaining good correlation over a significant load range, but in minimizing any error sources in the speckle translations.

5.2 Low Temperature

It is necessary to determine the basic characteristics of the system in a relatively benign test environment before exploring the upper limits of the technique. Therefore, complete tests were performed at room temperature using a standard flat tensile specimen of Inconel 600. Tests were conducted measuring uniaxial strain along the load axis, as well as biaxial strains using the optical rosette measurements.

The basic procedure of the two-dimensional technique is to first store a set of six reference speckle patterns with the specimen in the initial load state. The patterns are always generated in pairs, first from beam 1 and then from beam 2, at each angle a, b, and c. After storing these six digitized reference patterns, the specimen load is incremented and a set of six similar but shifted speckle patterns is recorded. Each set of corresponding reference and shifted patterns is correlated to determine the amount of shift the load induced, and strain is computed using equations (3.1.1) and (3.2.1-3).

As the load is increased, flexure and movement of the specimen causes the speckle patterns to migrate off the axis of the diode array. As mentioned in section 5.1, this makes it necessary to update the reference patterns at various points during the run. To assure maximum correlation accuracy during the Phase II testing, the reference patterns were updated before each load increment.

5.3 High Temperature

The specimen is raised to the test temperature using induction heating, and allowed to stabilize until no thermal expansion of the load components is observed (thermal expansion is indicated by load relaxation under slight tension of the specimen). This test verifies thermal equilibrium of the system before the run begins. The temperature is measured using an infrared pyrometer; a Proportional-Integral-Derivative (PID) controller adjusts the RF generator to maintain the specimen at a constant temperature.

For the high temperature tests the specimen is surrounded by a thermally insulating enclosure (fig. 5.3.1-a and b). The enclosure, fabricated from a refractory material, is designed to decrease nonuniformities in temperature around the specimen leading to dynamic air density fluctuations between the specimen and sensor. An optically flat fused silica window allows access to the test section while minimizing heat loss. The fluctuations in refractive index resulting from temperature induced airflow were observed to cause decorrelation in the Phase I testing. No indication of the fluctuations have been observed in the Phase II testing. Although this is in part due to the thermal enclosure, some optical system parameters are also believed to have an effect on speckle shifts caused by these fluctuations. Preliminary investigations indicate that a now planar wavefront may have diminished the speckle shifts caused by thermal variations.

6. RESULTS

6.1 System Tests

Several basic system responses are critical to the success of the measurements. Among these are insensitivity to rigid body motion, and stable or repeatable correlations.

Referring to requirement 2 in section 3.1, the relative sensitivity of the system to rigid body motion is inversely proportional to the radius of curvature L_S of the laser beam at the specimen. By positioning the beam waist at the specimen surface, the radius of curvature approaches infinity and error terms go to zero. This is observed by translating the specimen on a stage and verifying that the speckle shifts from beam 1 and beam 2 cancel. Successful cancellations occurred for translations along both the $\hat{x}$ and $\hat{z}$ directions. The maximum cancellation is of course limited by decorrelation of the signals. If the superposition of the reference and shifted laser spots on the specimen is not within roughly 50 percent, the visibility of the correlation peak is diminished and the shift cannot be determined directly.

Repeatability of the speckle correlations are a test of the stability of the optical and electronic systems. By recording a succession of speckle patterns and observing each correlation output, these stabilities are determined. At low temperature, the repeatability varies from 0 to 2 diodes over time. An uncertainty of one diode is attributed to the correlation resolution, and the remaining variation is believed to be caused by electronic noise introduced by the custom electronics. High temperature stability varies from 0 to 8 diodes over a number of minutes (at 750°), however, a typical short term variation remains around 0 to 2 diodes. The added variation over time seems to be due

to thermal loads in the specimen as the induction heater cycles up and down maintaining the temperature setpoint. In other words, the large variations at high temperature appear to be true strain measured by the system. This high temperature stability shows a marked improvement over the Phase I system. Total decorrelation occurred above 450° during Phase I testing.

6.2 One-Dimensional Tests

The one-dimensional measurements acquire data along axis b, parallel to the load axis. The measurements of Young's modulus are shown to be improved over the Phase I results due to the improved rigid body motion error cancellation. Figure 6.2.1 shows one-dimensional stress-strain curves at room temperature. One set of data indicates the strains measured while applying load and the other set represents the strain measured while backing the load down. Little or no systematic or random walk-off (cumulative error) is observed over the run, as verified by the minimal variation between the curves. This indicates that the incremental shift summing technique introduces errors of essentially zero mean. The value of Young's modulus given by these data is 228 MPa, which agrees with the handbook value to within 10 percent.

Figure 6.2.2 shows a one-dimensional run at 650 °C. Excellent linearity is observed, with no rigid body motion errors. The measured value of Young's modulus is 165 MPa. This agrees to two significant figures with the handbook value at 650°.

Note the difference in the data near the origins of figures 6.2.1 and 6.2.2. There is a bend in the data of figure 6.2.1 due to specimen movement that was eliminated in subsequent runs by further increasing the radius of curvature L_s. Figure 6.2.2 shows stress-strain behavior at the origin that is now linear to within the resolution of the system. Note also in figure 6.2.1 that the strain anomaly reversed as the rigid body motions reversed during the load down cycle. This demonstrates that the error was not random, but a response of the system.

The upper load limit of this run, as with all of the runs above 600°, is determined by the induction heating coil geometry. Due to the need for optical access to the test section, which is in the middle of the specimen, the induction coils are concentrated more near the ends of the specimen. The magnetic field is likewise concentrated near the ends, so this localized coupling heats the specimen ends more than the middle. This temperature profile is expected. The problem, however, is that as the load is increased during a run the ends of the specimen go into plastic strain before the test section. The load relaxes faster than the response of the system, and the subsequent data points are corrupted. The thermally insulating enclosure around the specimen serves to raise the temperature at which this effect begins by making the temperature distribution along the specimen more uniform.

6.3 Two-Dimensional Tests

Figure 6.3.1 shows plots of the first and second principal strains at a point, over a load-up and load-down cycle at low temperature. Young's modulus was measured to be 214 MPa (a 3 percent deviation from the handbook value of 207 MPa). The calculated Poisson's ratio ν is 0.32, and the mean angle of the principle strain axes $\bar{\phi} = 2°$. The handbook value of Poisson's ratio for Inconel 600 is 0.29 at room temperature, indicating agreement within 10 percent.

Figure 6.3.2 demonstrates the high temperature two-dimensional capabilities of the system at 750°. The good linearity of the principal strain moduli indicate stability of the system. Young's modulus is measured to be 124 MPa, which differs from the published value by -22 percent. The slope of the transverse axis ϵ_1 is unrealistically high, however, leading to a ν of 0.46 (the estimated value for this material is 0.31). This discrepancy is believed to be due to load relaxation occurring during acquisition of the three strain components, as mentioned in section 6.2. Although in this case each component of strain is accurate at its instantaneous load, each component in the set represents a slightly different load state. The time required to rotate the goniometer and read a set of 6 speckle patterns is 10 sec. This response time, therefore, defines the quasi-static two-dimensional measurement requirement for the system. In this test $\bar{\phi}$ = 15°, which does not coincide with the mechanical axis of the tensile machine. Although there is a variation in angle over the load range (ϕ approaches zero degrees as the load is increased), ϕ is consistently positive. It may be that uneven heating of the specimen ends caused the true load axis to shift and the orientation of the principle strain axes to rotate, but the apparent rotation is probably connected to the transverse strain error.

The highest temperature at which tests were conducted (750°) is the maximum steady temperature to which the RF induction heater has been able to raise the test section, rather than the upper limit of the technique. No inherent limits relating to temperature have been observed using the Phase II optical system.

7. ERROR ANALYSIS

The following is a discussion of the errors in the speckle shift technique as implemented by the Phase II system. An analysis of the Phase II system results shows an improvement in accuracy over the Phase I system, as discussed in section 7.1, while maintaining about the same resolution. The error terms introduced in the Phase I report comprise a subset of the Phase II error terms. The additional Phase II terms are listed in section 7.2.

7.1 Rigid Body Motion Cancellation

Cancellations of speckle shifts resulting from translations and rotations of the specimen are achieved by limiting the geometry of the optical setup, and by introducing a relatively large radius of curvature of the laser beam at the gauge location. Fine adjustment of the laser beam path, and alignment of the specimen and line scan camera eliminates most terms of error. The lens used to position the beam waist at the specimen surface then provides a nearly planar wavefront, effectively cancelling the remaining rigid body motion error in the speckle shifts. Cancellation of translation terms has been demonstrated up to the decorrelation limit of the system.

To achieve maximum cancellation, however, no movement of the specimen is allowed while each speckle pattern pair is recorded, as stated in section 4.2. On a similar note, it is important to obtain all three components of strain before relaxation of the load occurs; the strain components must of course be based on the same load state of the specimen.

7.2 Systematic Error

Two parameters affecting the resolution of the system have been changed compared to the Phase I system. The parameter L_o has been increased to 1.0 m, increasing the resolution; at the same time, the angle θ has been decreased to 30°, decreasing the resolution. The optical resolution determined by unit shift and other system constants is given by equation 7.2.1.

$$\text{resolution} = \frac{\text{diode spacing}}{2L_o \sin(30°)}$$

$$= \frac{15\ \mu m}{2 \times 1\ m \times 0.5}$$

$$= 15\ \mu\epsilon \qquad (7.2.1)$$

The net effect of the two changes is to leave the basic resolution virtually the same as in Phase I.

The total differential equation describing the error in the system is

$$d\epsilon_{xx} = \frac{-d\Delta A_x}{2L_o \sin(\theta)} + \frac{dL_o}{L_o}\epsilon_{xx} - \frac{d\theta}{\tan(\theta)}\epsilon_{xx}$$

For the absolute shift method of measuring strain, this leads to a theoretical uncertainty of ±15 μ ±0.9 percent of the strain reading. This uncertainty varies with the design parameters of the system. The error that occurs in a real test situation is often larger than this over the course of a run, and depends on the accuracy of the cross-correlations used to determine the speckle field shifts. Partial decorrelation due to off-axis speckle shifts (shifts along the Y axis) often occurs during a load cycle. By frequently updating the reference speckle patterns the decorrelation effects can be minimized, but not necessarily before an error in A_X occurs.

The sensitivity to decorrelation caused by A_Y is decreased by using a taller photodiode array. A diode height of 300 μm is used in Phase II. The correlation requirement of

$$A_Y << \left[\frac{1.22\lambda L_o}{\omega} + \text{sensor height}\right] \qquad (7.2.3)$$

where λ is the laser wavelength and ω is the spot size, corresponds to $A_Y << 1.3$ mm.

Since the two-dimensional measurements are, physically, an extension of the one-dimensional technique, two-dimensional measurements add no systematic errors. That is to say, each strain component used to calculate the two-dimensional strains is still a one-dimensional measurement. However, by using three measurements in the calculation of the principal strains, the error is of course increased. The magnitude of the total error is calculated from the total differential equations (7.2.4) and (7.2.5).

$$d\epsilon_1 = \left(\frac{\partial \epsilon_1}{\partial \epsilon_a}\right) d\epsilon_a + \left(\frac{\partial \epsilon_1}{\partial \epsilon_b}\right) d\epsilon_b + \left(\frac{\partial \epsilon_1}{\partial \epsilon_c}\right) d\epsilon_c \qquad (7.2.4)$$

$$d\epsilon_2 = \left(\frac{\partial \epsilon_2}{\partial \epsilon_a}\right) d\epsilon_a + \left(\frac{\partial \epsilon_2}{\partial \epsilon_b}\right) d\epsilon_b + \left(\frac{\partial \epsilon_2}{\partial \epsilon_c}\right) d\epsilon_c \qquad (7.2.5)$$

After determining the partial derivatives from the principal strain equations, the total differential equations become

$$d\epsilon_1 = \frac{1}{2}\left[1 + \frac{2(\epsilon_a - \epsilon_b)}{\sqrt{(\epsilon_c - \epsilon_a)^2 + (2\epsilon_b - \epsilon_a - \epsilon_c)^2}}\right] d\epsilon_a + \left[\frac{(2\epsilon_b - \epsilon_a - \epsilon_c)}{\sqrt{(\epsilon_c - \epsilon_a)^2 + (2\epsilon_b - \epsilon_a - \epsilon_c)^2}}\right] d\epsilon_b + \frac{1}{2}\left[1 + \frac{2(\epsilon_c - \epsilon_b)}{\sqrt{(\epsilon_c - \epsilon_a)^2 + (2\epsilon_b - \epsilon_a - \epsilon_c)^2}}\right] d\epsilon_c \qquad (7.2.6)$$

and

$$d\epsilon_2 = \frac{1}{2}\left[1 - \frac{2(\epsilon_a - \epsilon_b)}{\sqrt{(\epsilon_c - \epsilon_a)^2 + (2\epsilon_b - \epsilon_a - \epsilon_c)^2}}\right] d\epsilon_a - \left[\frac{(2\epsilon_b - \epsilon_a - \epsilon_c)}{\sqrt{(\epsilon_c - \epsilon_a)^2 + (2\epsilon_b - \epsilon_a - \epsilon_c)^2}}\right] d\epsilon_b + \frac{1}{2}\left[1 - \frac{2(\epsilon_c - \epsilon_b)}{\sqrt{(\epsilon_c - \epsilon_a)^2 + (2\epsilon_b - \epsilon_a - \epsilon_c)^2}}\right] d\epsilon_c \qquad (7.2.7)$$

where

$$d\epsilon_{a,b,c} = \pm 15\ \mu\epsilon \pm 0.009 \times \epsilon_{a,b,c} \qquad (7.2.8)$$

The overall error is dependent on the magnitude of strain components $\epsilon_{a,b,c}$. Although never observed, a worst case error estimate of three times the strain error of the greatest strain component can be calculated using equations (7.2.6-8):

$$d\epsilon_{1,2} = \pm 3 \times [15\ \mu\epsilon \pm 0.009 \times \epsilon_{max}] \qquad (7.2.9)$$

8. CONCLUSIONS

One-dimensional and two-dimensional strain measurements have been demonstrated using the speckle shift technique. The validity of applying conventional rosette techniques to the optical system has been shown. Stable speckle patterns have been recorded at temperatures up to 750 °C with good autocorrelation characteristics. Linear stress-strain relationships have also been measured to this temperature. This maximum temperature is determined by the available heating power, and is not the temperature limit of the optical technique. The requirement for optical access between the induction coils caused uneven heating of the specimen. The localized high temperatures caused difficulties in obtaining accurate two-dimensional measurements. Since the data for the one-dimensional measurements were acquired in milliseconds no relaxation error is observed. A general rule for obtaining high accuracy, which applies to virtually all measurements, is that the specimen state must be stable to within the resolution limit over the duration of the measurement. One cure for the two-dimensional relaxation effect would be to change the specimen geometry to decrease the stress at the higher temperature areas. A radiative heater could be used to provide more uniform heating. Ideally, acquiring the data faster would minimize the effects of a dynamic test situation. This would, however, require substantially more complicated optics.

The sensitivity of the system to changing refractive index gradients seems to be decreased by changes in the optical parameters of the system. The index gradients themselves have been decreased by enclosing the specimen in a thermally insulating box.

Rigid body motion errors in excess of the system resolution were successfully cancelled, up to the decorrelation limit of the optical system. The improvement in error cancellation is due to an increase in the radius of curvature of the laser beam at the specimen. The sensitivity of the system to decorrelation was decreased by using a taller photodiode array. A smaller spot size reduces the gauge length of the measurement, but at the same time reduces the maximum speckle shift per strain point. Imprecise loading and excessive shifts due to the fatigue testing machine contribute to the error margin during tests before L_s was maximized. After adjustments were made to L_s decorrelation still made measurements tedious at times, but little or no rigid body motion error was observed. A precision load machine will allow better alignment of specimens and consistency between runs. Overall, the speckle shift technique shows very good promise as a high temperature optical strain gauge. Measurement of one-dimensional strains into the plastic regime have been demonstrated previously. Two-dimensional plastic strains require a faster beam rotation system or a more complex six-beam optical switching setup.

Future work will further decrease the sensitivity of the system to decorrelation due to A_Y translations by recording two-dimensional speckle fields. A high speed hardware correlator will keep the additional computational requirements within a very reasonable timeframe.

REFERENCES

1. Lant, C.T.; and Qaqish, W.: Optical Strain Measurement System Development - Phase I. NASA CR-179619, 1987.

2. Yamaguchi, I.: A Laser-Speckle Strain Gauge. Phys. E. Sci. Instrum., vol. 14, no. 11, Nov. 1981, pp. 1270-1273.

3. Murray, W.M.: Rosette Analysis. Massachusetts Institute of Technology Lecture Series, July 6-10, 1965.

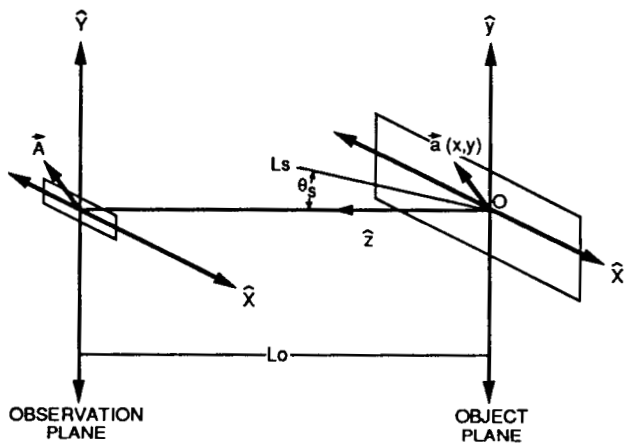

Figure 3.1.1. - Simplified coordinate system.

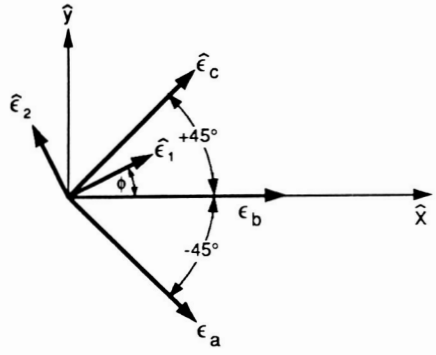

Figure 3.2.1. - Rectangular rosette diagram.

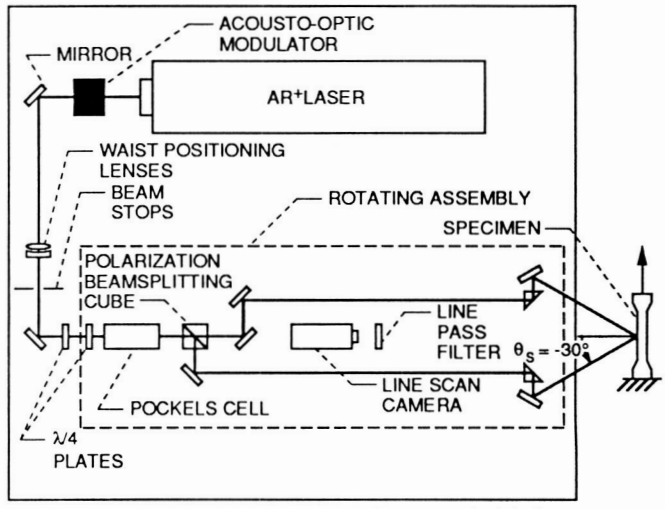

Figure 4.1.1. - Schematic of the Phase II optical design.

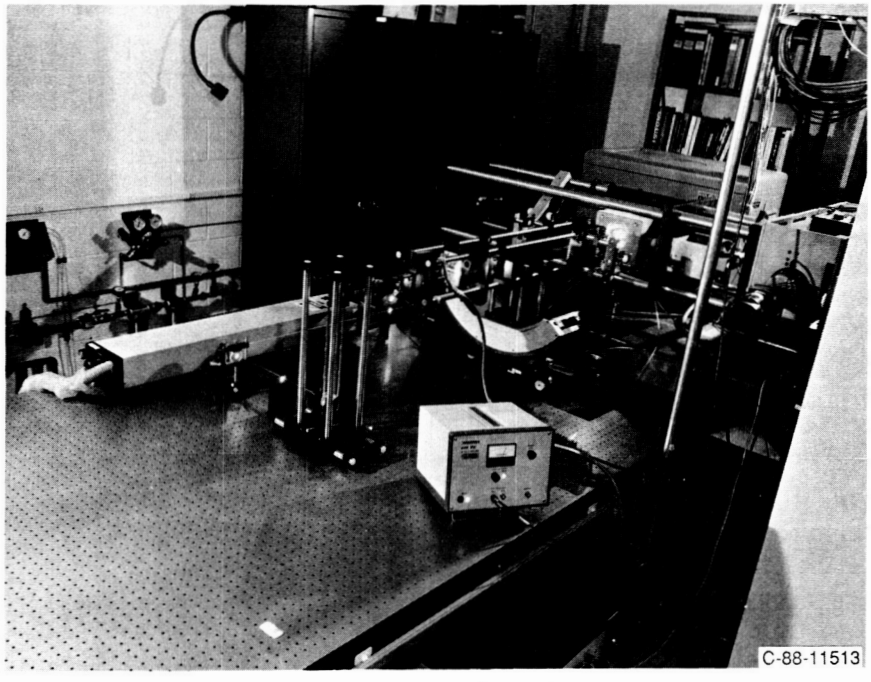

Figure 4.1.2. - Phase II test setup.

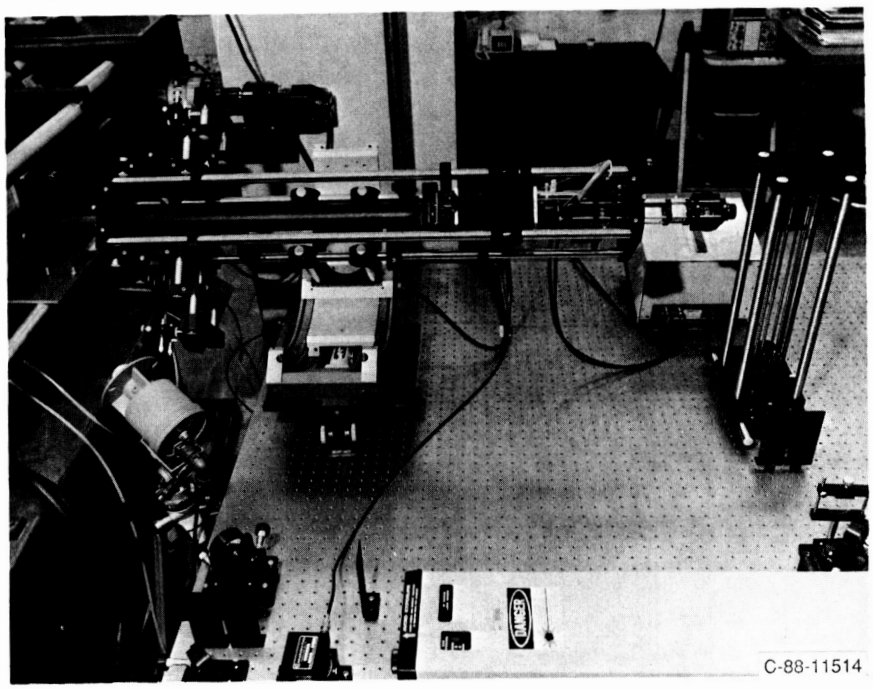

Figure 4.1.3. - Rotating assembly.

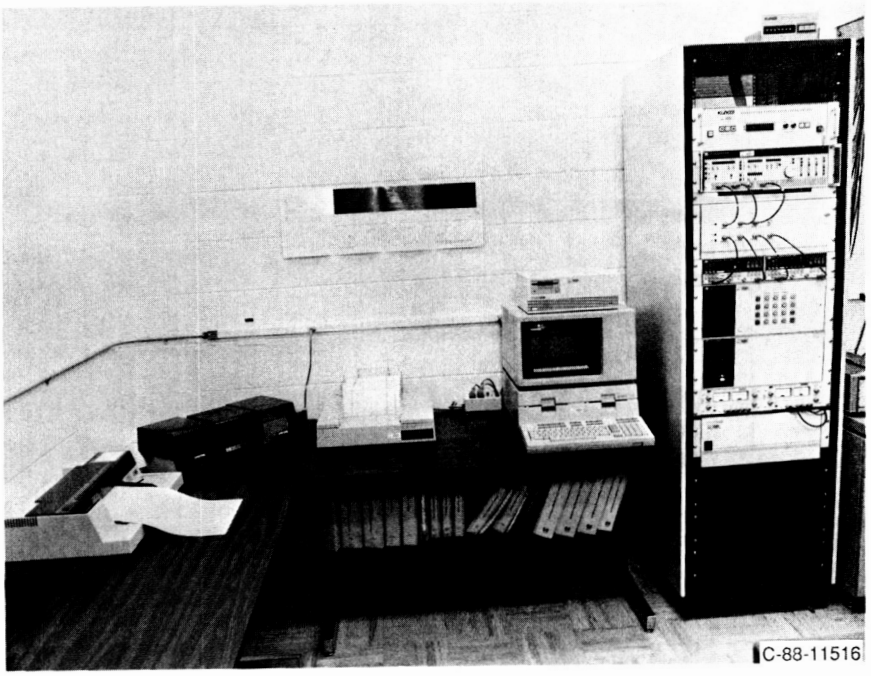

Figure 4.3.1. - Computer system.

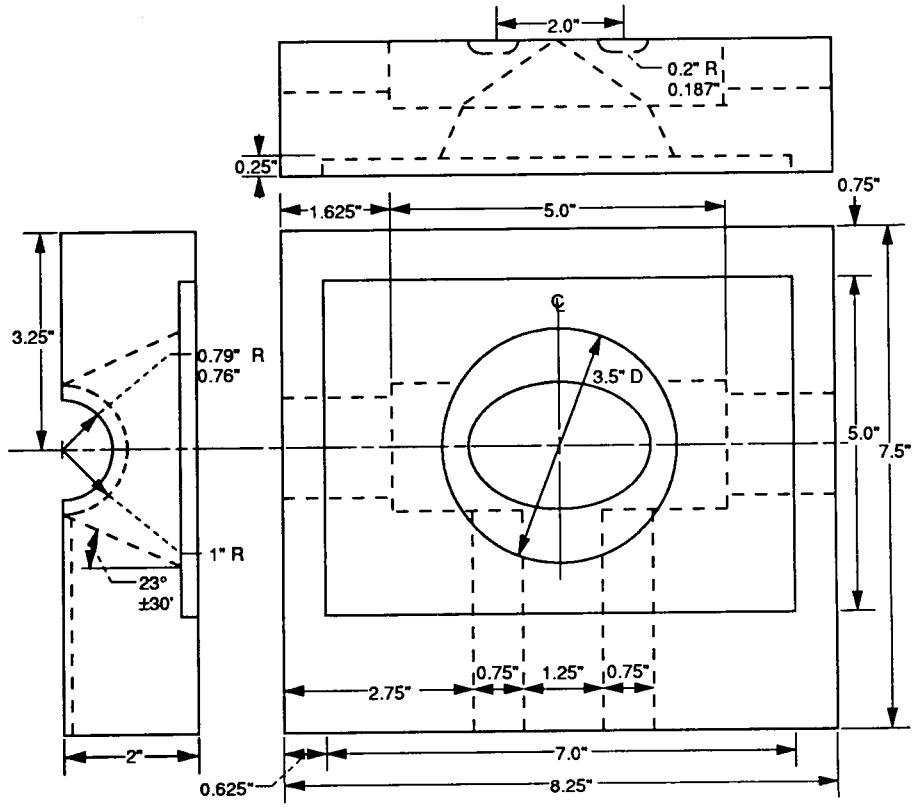

Figure 5.3.1 (a) - Front half of enclosure.

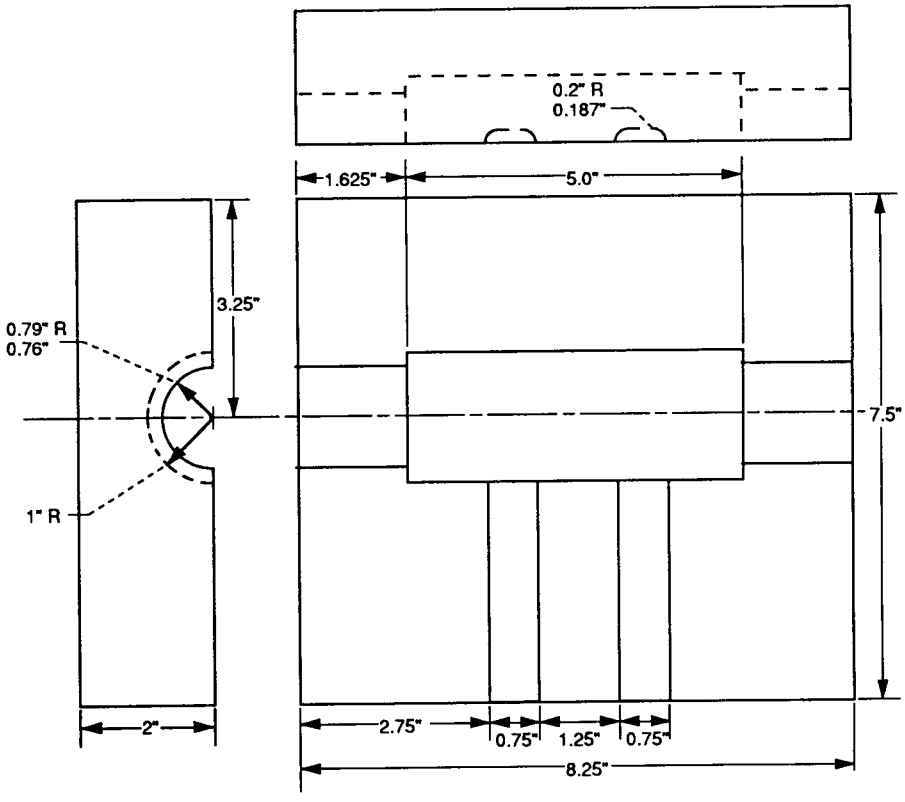

Figure 5.3.1 (b) - Rear half of enclosure.

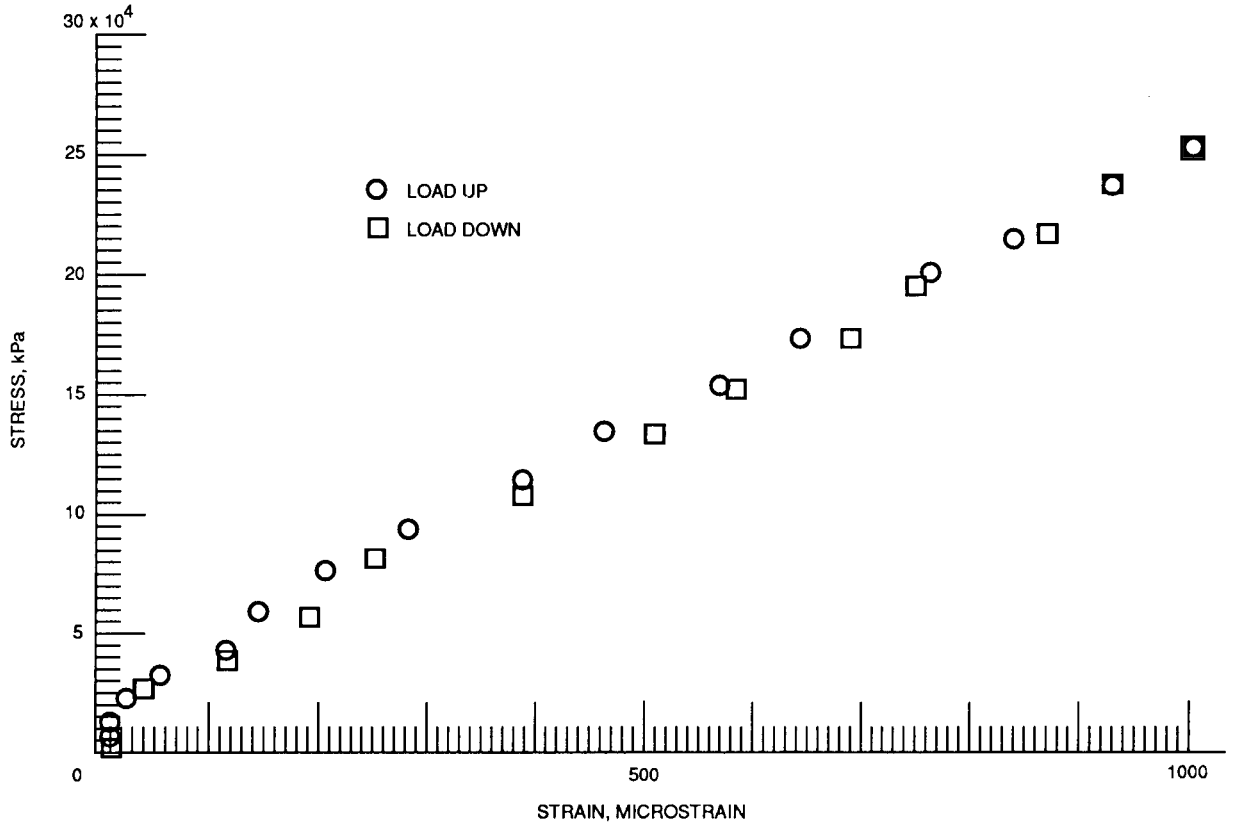

Figure 6.2.1. - 1-D run at room temperature.

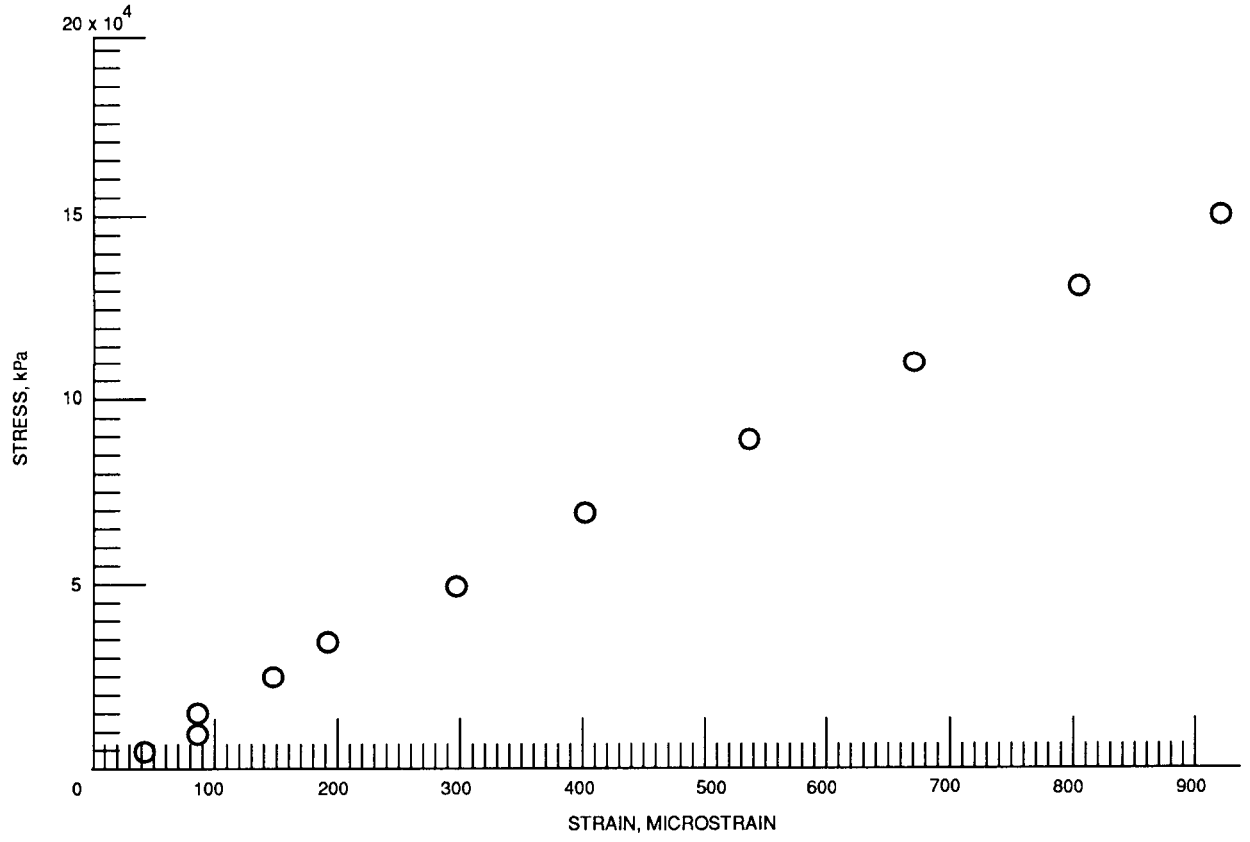

Figure 6.2.2. - 1-D run at 650 °C.

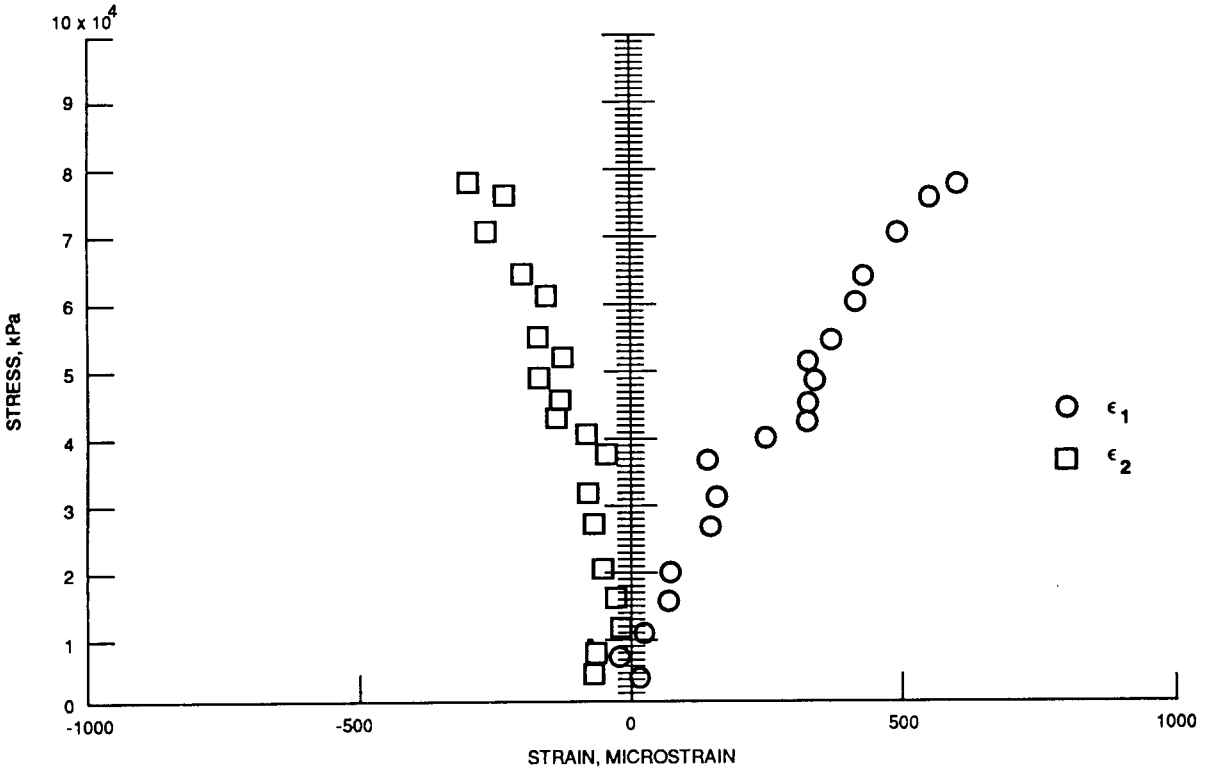

Figure 6.3.2. - 2-D run at 750 °C.

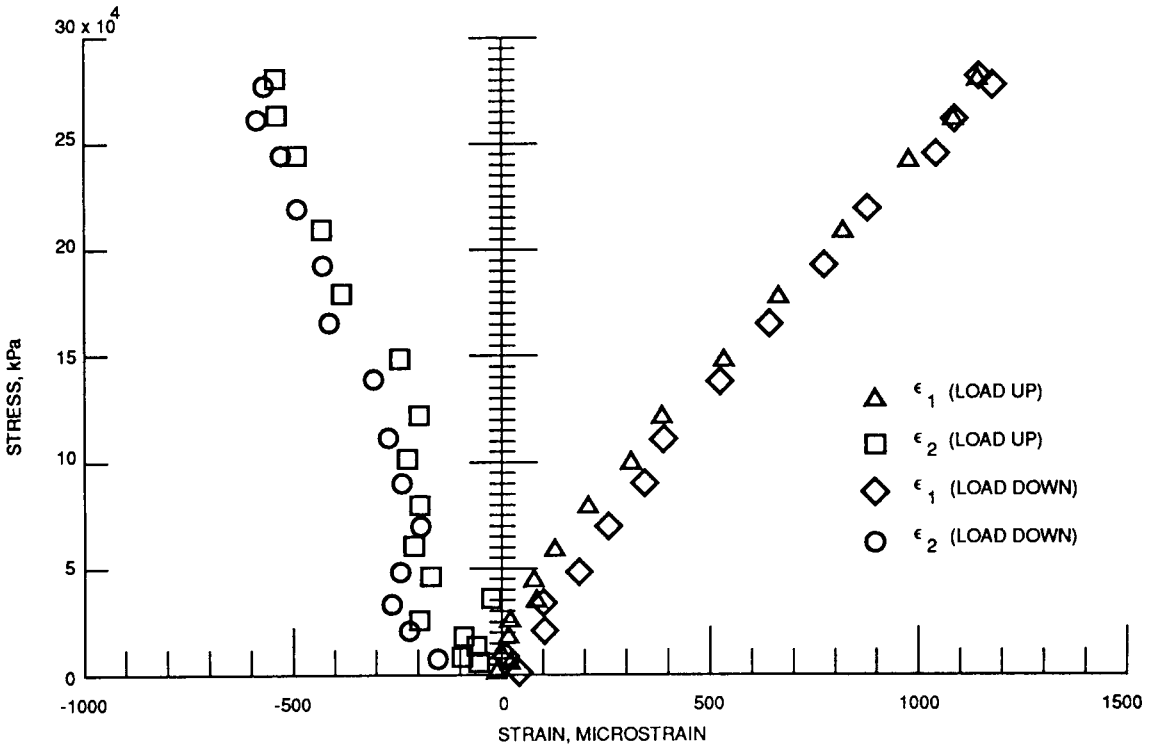

Figure 6.3.1. - 2-D run at room temperature.

NASA
National Aeronautics and Space Administration

Report Documentation Page

1. Report No.	2. Government Accession No.	3. Recipient's Catalog No.
NASA CR-185116		

4. Title and Subtitle
Two-Dimensional High Temperature Optical Strain Measurement System—Phase II

5. Report Date
July 1989

6. Performing Organization Code

7. Author(s)
Christian T. Lant

8. Performing Organization Report No.
None (E-4923)

10. Work Unit No.
582-01-11

9. Performing Organization Name and Address
Sverdrup Technology, Inc.
NASA Lewis Research Center Group
Cleveland, Ohio 44135

11. Contract or Grant No.

13. Type of Report and Period Covered
Contractor Report
Final

12. Sponsoring Agency Name and Address
National Aeronautics and Space Administration
Lewis Research Center
Cleveland, Ohio 44135-3191

14. Sponsoring Agency Code

15. Supplementary Notes
Project Manager, John P. Barranger, Instrumentation and Control Technology Division, NASA Lewis Research Center.

16. Abstract

A laser speckle strain measurement system with two-dimensional measurement capabilities has been built and tested for high temperature applications. The 1st and 2nd principle strains at a point on a specimen are calculated from three components of one-dimensional strain. Strain components are detected by cross-correlating reference and shifted speckle patterns recorded before and after straining the specimen. Speckle patterns are recorded by a linear photodiode array camera. Accurate strains have been measured at temperatures up to 650 °C. Stable speckle correlations and linear stress-strain relations have been demonstrated up to 750°. The resolution of the system is 15 $\mu\epsilon$, with a gauge length less than 1 mm.

17. Key Words (Suggested by Author(s))	18. Distribution Statement
Laser speckle; 2-D optical strain measurement; High temperature strain measurement; Correlation; Remote sensing	Unclassified – Unlimited Subject Category 35

19. Security Classif. (of this report)	20. Security Classif. (of this page)	21. No of pages	22. Price*
Unclassified	Unclassified	22	A03

*For sale by the National Technical Information Service, Springfield, Virginia 22161